

No. Registrasi: 0702010113010475

Material Researches and Energy Engineering

**Edited by
Yijin Wu**

Table of Contents

Preface and Organizing Committee

Chapter 1: Polymer Materials and Plastic Materials Properties

Experimental Study on Controlled Impact Effect in Plastic Deformation Processes T. Penchev, D. Karastojanov and I. Altaparmakov	3
Synthesis of Silver Nanocomposite with Poly(vinylpyrrolidone) and Poly(4-vinylpyridine) for Antimicrobial Activity P. Parashar	9
Modernization of Technology and Organization of Production of Triethylaluminium Co-Catalyst for Olefin Polymerization R.V. Tumasev, O.A. Arkatov, M.A. Goryaynov, V.K. Dudchenko, E.A. Mayer and A.N. Pestryakov	15
A Study of Performance on Anti-Pollution Flashover Coating Based on Composite Room Temperature Vulcanized Silicone Rubber M.X. Guo, S.H. Xue, Y.Y. Zhang, Z.Y. Wang and W.Z. Zhang	20
Research of Synthesis and Heat Resistance on Lactic Acid-Styrene-Maleic Anhydride Copolymer J.J. Shang, L.N. Jiang, D.Q. Li and X.Y. Zhu	25
Effect of Thermal Treatment on the Morphological Structure and Properties of Polyester Hollow Staple Fibers W.M. Wang, B. Yu, H.Z. Su and Z. Zhang	30
Effect of $Co^{60}\gamma$ Ray Irradiation on Thermoplastic Corn Starch Plastic H. Tang, H.T. Jiang, B. Guo and P.X. Li	34
Effect of Higher Thermoplastic Starch Content on TPS/LDPE Plastics H. Tang, H.T. Jiang, B. Guo and P.X. Li	38

Chapter 2: Steel, Iron, Metals, Alloys and their Applications

The Research of the Impact of Dynamic Analysis from the Stiffness of the Light Steel Floor of the Steel Frame C.X. Gong and C. Xi	47
Analysis and Calculation of Carbon Content in Austenitizing of Cast Iron W.B. Gong, Y. Zhang and G.Y. Xiang	52
Al Vacancy Induced Room-Temperature Ferromagnetic in Un-Doped AlN H.H. Ren, R. Wu, J.K. Jian, C. Chen and A. Ablat	57
Deformation Twinning in Hadfield Steel A.A. Yeleussizova, M.K. Skakov, A.M. Zhilkashinova and O.V. Rofman	62
Purification Efficiency and B Removal of Polysilicon during its Solidification from a Si-Al-Sn Melt S.R. Wu, F.M. Xu, J.Y. Li, Y. Tan and Y.Q. Li	68
Simulation of Microstructure and Properties of As-Cast Al Alloys X.M. Li, J.J. Yu and J. Yu	72
Finite Element Analysis of Fretting Wear for Nuclear Inconel 690 Alloy J.N. Mei, F. Xue, L. Huang, Z.X. Wang, G.D. Zhang, G.G. Shu, J.S. Li and H.Z. Fu	77
Prediction of the Magneto-Resistance of $La_{0.65}Ca_{0.35}MnO_3$ and $La_{0.8}Sr_{0.2}MnO_3$ via Temperature and Magnetic Field N. Zhu and Y.J. Liu	83
The Shielding Gas Influence on the Laser Beam Welding of 2205 Duplex Stainless Steel J. Bárta, T. Vrtochová and P. Krampot'ák	89
An Investigation into Microstructures and Properties of 7075-T6 during Friction Stir Welding W. Wu and D.J. Chen	94

Crystallographic and Electrochemical Performances of La_{0.73}Ce_{0.27}Ni_{3.25+x}Mn_{0.35}Al_{0.15}Cu_{0.75}Fe_{0.25} (x = 0-0.75) Hydrogen Storage Alloys Y. Zhou, X.Y. Peng, L.Q. Ji and Y.P. Fan	98
Effect of Cerium-Rich Mischmetal Addition on the Microstructure and Properties of Die-Cast Mg-Alloys D.P. Jiang and Z.X. Yao	103

Chapter 3: Building Materials and Constructions Engineering

Experimental Research of Sulfate Corrosion Resistance of Fresh Concrete with Fly Ash Q.Y. Dong, Y.H. Zhang, L.P. Feng, D.B. Jin, J.S. Zhang and C.C. Wang	109
The Role of Building Materials Development in Constructing Form Evolution S.C. Sun and Z.S. Wei	117
Total Pressure Gradient Incidence on Hygrothermal Transfer in Highly Porous Building Materials K. Abahri, R. Belarbi, N. Oudjehani, N. Issaadi and M. Ferroukhi	124
Coupled Timber – Concrete Ceiling Using Bonded Shear Connectors R. Cajka and K. Burkovic	130
Study on the Combustion Performance of the Building Insulation Materials Y.F. Chen, S. Zhuang and L. Yang	136
Stress Discontinuities in Normal Stress Distribution of Adhesively Bonded Beams X.C. He	140
Applications of High-Efficiency Insulations for Building Energy Saving Y.C. Kwon	144
Investigation on Seismic Behavior of Recycled Aggregate Concrete Structures under Dynamic Loadings C.Q. Wang	149
Study on the Anti-Static Desulphurization Gypsum Fiberboard Y.L. Liu, C.F. Tang, W.H. Shen, J.W. Han and H.S. Du	156
Experimental Research of Concrete Resistance to Freezing-Thawing by Double Mixing Steel Slag J.L. Shang and X. Li	161
Special Nylon Fabric as a New Material for Reinforcing Cement Composite P. Teymouri, M. Zargarán and N.K.A. Attari	167
Advanced Fiber-Reinforced Composite Materials for Marine Applications B. Ertuğ	173
The Development and Application of Non-Shrinking Composite Silicate Insulation Material Y.L. Zhan, H.Y. Chen, X.H. Hou and F. He	178
Experimental Investigations on Mechanical Properties and Fire Resistance of Steel-Polypropylene Hybrid Fiber Reinforced Concrete D. Ouyang, L.J. Kong, H. Fu, L.L. Lu, L. Liao and C.W. Huang	182
Analysis and Experiment on the Chuck for Equivalent Strength Connection of Wire Rope H.Z. Chen, X.Y. Zhang, W. Li, Y.L. Wang and Q.L. Zhang	188
Study on Bending Behaviors of Φ500 PHC Pile X. Xia, H. Xu, H.D. Xu and R.J. Gu	193
Static Test and Bond Stress Analysis of the New Kind of Anchor for CFRP Tendon B. Chen and S.Q. Li	198

Chapter 4: Bio, Chemistry and Medical Materials and Engineering

Selective Transport Capacity for K⁺ and Ca²⁺ over Na⁺ of Leaf Sheath is Correlated with Salt Tolerance of Energy Plant Sweet Sorghum T.L. Ding, J. Song, H. Fan, H.D. Wu, Y. Liu, S.C. Zhang and B.S. Wang	207
The Comparative Study of NO_x Oxidation Using PMS Catalyzed by Co₃O₄/GO and Mn₃O₄/GO X.Z. Sun and D.X. Li	215

Analysis Content of 1-methyl-3-butyl Imidazole Tetrafluoroborate in Water by UV-Spectrum	
Y.Y. Song, P. Tian and L. Yu	219
Study on Synthesis and Performance of Collagen-Modified Polylactide	
L.L. Liu, R.X. Su and X. Li	223
Product Distributions of Benzene Alkylation with Propylene Estimation Using Artificial Neural Network (ANN)	
X.Y. Sun and S.G. Xiang	227
An Improved Algorithm Based on Retinex Theory for X-Ray Medical Image	
W.B. Wang, L.J. Zhou and L. Fei	233
The Kinetic Model Including Singlet Oxygen and Ozone in Hydrogen-Air Mixture	
Y.N. Chang, C.H. Wang and T.G. Cheng	239
Effect of Ionic Liquid Pretreatment on the Enzymatic Saccharification of Sugarcane Bagasse	
W. Liao, Z.M. Wang and B.J. Li	246
Degradation Kinetics of Coconut Chaff in Subcritical Water	
F.L. Xu, X.P. Bai, L.J. Li and Y.Y. Jia	252
Static Stress Distribution in Microvessel Wall with a Layered Model	
F.R. Gao, X.G. Xi, Y.Y. Gao and Q.Z. Zhang	258
The Requirements of Structure and Properties of Palm Fiber Mattress	
C.Y. Cai, Z.H. Wu, X. Liu and Y.Q. Li	264
Study of a Novel High-Strength Antibacterial Dental GIC Restorative	
D. Xie, Y.M. Weng and L. Howard	270
The Reverse Water-Gas Shift Reaction and the Synthesis of Mixed Alcohols over K/Cu-Zn Catalyst from CO₂ Hydrogenation	
S.G. Li, H.J. Guo, H.R. Zhang, J. Luo, L. Xiong, C.R. Luo and X.D. Chen	275
The Binary Vapor-Liquid Phase Equilibrium of Citronella Oil under High Vacuum	
Q. Chen, L.L. Gu and Z.H. Zhang	281
Anti-Oxidation Stability and its Mechanism of Rapeseed Biodiesel	
J. Wu, B.S. Chen, J.H. Fang and J. Wang	287
Modeling of Oligomerization of C₉ Fraction of Petrol Pyrolysis	
A.A. Lyapkov, E.I. Ionova, V.G. Bondaletov and A.N. Pestryakov	292
Laboratory Experimental Research on Promoting Aquathermolysis of Heavy Oil with the NaNO₂/NH₄Cl Exothermic System	
L. Dong, Y.C. Cai, Y.J. Liu, K.M. Xu, D.X. Chen, X.W. Kong and F.J. Zhao	297
A Review on Biodiesel Synthesis Using Catalyzed Transesterification Base Ionic Liquids as Catalyst	
B.Y. Han, W.D. Zhang, Y.B. Chen, F. Yin, S.Q. Liu and X.L. Zhao	303
The Luminescence of Rare Earth Composite Micelles in Different Polarity	
Z.Y. Li, Z.J. Xue and L.J. Kong	309
Pyrolysis Kinetics Equation of Larch Bark	
H.S. Du, X.Y. Li, X.Y. Ren and Y.X. Han	313
The Influence of Environment Factors on Lubricants Biodegradation by Orthogonal Design	
J. Wang, B.S. Chen, J.H. Fang, J. Wu and L. Mei	319

Chapter 5: Nanomaterials and Nanotechnologies

Effect of Calcining Temperatures on the Morphology and Crystallinity of Strontium Doped Hydroxyapatite Nanopowders	
C.M. Mardziah, I. Sopyan, N.R. Nik Roselina and K.M. Hyie	325
Optical Property of Pyramidal-Substrate with Nano Porous Layer	
Y.H. Tang, W.J. Wang, C.L. Zhou, S. Zhou, Y. Zhao, J.M. Fei, H.B. Cao, J.W. Chen and B.J. Yan	331
Nanostructural Materials for Dye-Sensitized Solar Cells	
C. Cheng, C.C. Ho, C.T. Wu and F.H. Ko	337
Visible-Light Illumination Enhanced Hydrogen Evolution on CuO Modified TiO₂ Nanotube Arrays/Ti Electrocatalyst	
Z.X. Yan, Z.H. Xu and L.H. Zhu	343

Preparation of Graphene/Pd Nanoparticle Composites and their Hydrogen Storage Z.L. Hu, Y.F. Chen, N. Li, W. Zhang, H. Chen and W.Q. Gong	349
Study of Nonlinear Effect about Laser-Induced Processes of Nanodispersed Gold in Mineral Association N.A. Leonenko, E.A. Vanina, G.G. Kapustina and E.M. Veselova	355
Supported Iron Nanoparticles for Removal of Pentachlorophenol in Water R. Cheng, X. Zheng, G.Q. Li and J.L. Wang	359
Physical Properties Study of TiO₂ Nanoparticle Synthesis via Hydrothermal Method Using TiO₂ Microparticles as Precursor M.H. Razali, M.N. Ahmad-Fauzi, A.R. Mohamed and S. Sreekantan	365
The Preparation and Visible Light Photocatalytic Activity of TiO₂/Co²⁺ Nanofibers C.X. Xu, Y.K. Shi, M. Zhou, X. Qian and X.F. Ye	371
Performance Research of PUE/Modified Nanosilicon Carbide / Carbon Nanofibers Q.Z. Wen, Q. Cheng and J.H. Zhu	376
Structural Shifting and Electronic Properties of Stone-Wales Defect in Armchair Edge (5,5) Carbon Nanotube S. Jadi and A. Setiadi	380

Chapter 6: Manufacturing Materials and Engineering, Industry Engineering

The Wear Analysis of Chisel-Edge Ruling Tool for Diffraction Gratings J. Galantu	389
Synthetic Evaluation of Equipment Maintenance System Based on TOPSIS Method M.H. Yang, Y.C. Dong, L. Zhang, J. Du and Y.X. Liu	394
Computational Modeling of the Pulling Force in a Conventional Pultrusion Process P. Carlone and G.S. Palazzo	399
Development of Embedded Laser Marking Controller Based on ARM9 Y. Fang, D.Y. Wang, Q.W. Yu and Y.X. Wei	407
Macro-Micro Modeling Analysis for a Two-Steps Micro Reactor X.Y. Chen and H. Zeng	412
The Simulation and Analysis of Hydro-Pneumatic Suspension Performance Based on AMESim Z.L. Zhang, G.Q. Meng and R.Q. Dai	416
Gate Tunneling Current Predicting Model for Scaled NMOSFET Devices Z.C. Zhao, T.F. Wu, H.B. Ma, Q. Wang and J. Li	422
The Influencing Factors and Assessment Model of Fatigue Life of Shaft Y.Z. Yuan	427
LXI Precision Time Protocol Applied Research M. Li, C.P. Wang and Z.Q. Wang	432
Development of a Single-Cylinder Four-Stroke Free-Piston Generator Z.P. Xu and S.Q. Chang	436
New Control Strategy for High-Frequency Digital Inverter Power Supply Y.W. Wang	443
Multi-Feature Load Detection Algorithm C. Donciu, A.S. Ardeleanu and T. Marinel	448
A Low-Cost Head Supported Eye Tracker with High Precision J.C. Chen, S.Q. Ma and L.P. Zhao	455
Research on Filter Paper Splash Procedure of Raindrop Diameter Y.J. Huang and Y.Y. Huang	461
Core Conductive Yarn Based Integral Knitted ESD Garments Part I. Metallic Core Conductive Yarns Investigation C. Donciu	467
Core Conductive Yarn Based Integral Knitted ESD Garments Part II. Carbon Composite Yarns Investigation C. Donciu	474

Experimental Investigation on Thermal Performance of Flat Plate Heat Pipe with Intersected Micro-Grooves	
C. Wang, Z.L. Liu and G.M. Zhang	480
Co-Combustion of Paper Mill Sludge and Bituminous Coal in Air Using Thermogravimetric Analyzer	
Y.Z. Li, X.Q. Ma, Y.T. Tang and Z.L. Cai	487
Neutronic Performance of Small Long-Life Boiling Water Reactor Using Thorium as Fuel and the Addition of Protactinium as Burnable Poisons	
N. Trianti, Z. Su'ud, I. Arif and E.S. Riyana	495
Application of Modified CANDLE Burnup to Very Small Long Life Gas-Cooled Fast Reactor	
F. Monado, Z. Su'ud, A. Waris, K. Basar, M. Ariani and H. Sekimoto	501
Analysis on Even Mass Plutonium Production of Different Loading Materials in FBR Blanket	
S. Permana, N. Trian, A. Waris, Z. Suud, I. Mail and M. Suzuki	507
Irradiation and Cooling Process Effects on Material Barrier Analysis Based on Plutonium Composition of LWR	
S. Permana, N. Trian, A. Waris, Z. Suud, I. Mail and M. Suzuki	513
Preliminary Study of Safety Analysis of Pb-Bi Cooled Small Power Reactor with Natural Circulation	
N. Trian, A. Waris, S. Viridi and Z. Suud	519
Neutronic Design of Small Long-Life PWR Using Thorium Cycle	
M.N. Subkhi, Z. Su'ud and A. Waris	524
Desain Study of Pb-Bi Cooled Fast Reactors with Natural Uranium as Fuel Cycle Input Using Special Shuffling Strategy in Radial Direction	
Z. Su'ud, F.H. Irka, T. Imam, H. Sekimoto and P. Sidik	530
Comparisons of Alcohol Blending Fuels' Emission from a Laboratory Gasoline Engine	
T.N. Wu, Y.C. Hsu and T.S. Wu	536
Transient Fuel Injection Rate and Fuel Economy Prediction for a Vehicle Driven with FTP-75 Mode Using an ECU HILS	
C.H. Lee	543
Urban Low-Carbon Transport, Model of Pure Electric Vehicle Development Typical Research Based on Hangzhou Pure Electric Taxi Demonstration Operations	
F.S. Zhu, X.M. Chen, R.K. Ye and J.Q. Bao	549
Interference Characteristics Analysis of Power Electronics Devices Used in New Energy Vehicles	
Y.J. Guo, L.F. Wang and C.L. Liao	556
Comparative Study of the Hydrodynamic Performance of Shorter and Longer Blades in a Swirling Fluidized Bed	
V.K. Venkiteswaran, S. Anwar Sulaiman and V.R. Raghavan	560
An Approach to Calculate the Directions of Crystal Defects in Synchrotron Radiation Topography	
W.L. Yu, X.P. Jia and Q.X. Yuan	566
Response Function of Collimated Detector for Non Axial Detector-Source Geometry	
R. Wirawan, M. Djamal, A. Waris, G. Handayani and H.J. Kim	571
 Chapter 7: Power, Energy Materials and Engineering Applications	
Solar Refrigerating Systems	
I. Sarbu, E. Valea and C. Sebarchievici	581
Small Wind-Solar Hybrid Power Generation System Based on Multi-Agent	
J. Chang, Y. Peng and X.J. Feng	587
Small Multi-Agent Wind Solar Hybrid Power Generation System Design and Implementation	
J. Chang, Y. Peng and X.J. Feng	594
Smart Grid Construction Based on Perspective of the Development of Servicing Clean Energy	
J. Nie	600

A New High Voltage Transmission Lines Deicer Based on Vibrations Principle J. Nie	604
Analysis for Solar Array Radiation Receiving Characteristics on Stratospheric Airship K.W. Sun, G.M. Liang, K. Li and M. Zhu	608
Chinese Wind Energy Development Analysis and Construction Proposals Z.W. Bai	615
An Analysis about Wind Farm Construction Based on the Perspective of the Development of Ecological Environment Z.W. Bai	619
Analysis of Prestressed Concrete Tower for Wind Turbine Generator R. Cajka	622
Accommodation Capacity Analysis of the Large Scale PV Power Generation Access to Regional Power Grid T. Shi and H.L. Han	630
Temperature Dependent Study of Carrier Diffusion in Photon Enhanced Thermionic Emission Solar Converters Y. Yang, W.Z. Yang, W.D. Tang and C.D. Sun	634
Effect Study of Large-Scale PV Power Access to HVDC System H.L. Han, Z. Li, T. Shi and N. Chen	640
The Status Quo Analysis of New Energy Industry Standardization System in NingXia Province M.B. Li, P.Q. Yang and C.X. Mu	646
Mathematical Model and Numerical Experiment of Photovoltaic Water Pumping System K.Y. Wang and Q.S. Wang	653
High Efficiency MPPT Using Piecewise Linear Approximation and Temperature Compensation Y.Y. Yang, W.D. Yi and K.W. Jwo	658
Contingency Analysis Model of Electrical Power Systems Based on Central Angles from PMUs G.J. Lopez, J.W. Gonzalez, A.E. Diez, I.A. Isaac, H.A. Cardona and R.A. Leon	664
Research a Suitable Textbook to Educate High-Level Employees of the Wind Energy Industry in Taiwan S.H. Huang and C.S. Cheng	673
Theoretical Study of New Configuration of Photovoltaic/Thermal Solar Collector (PV/T) Design M.I. Fadhel, S.M. Sultan and S.A. Alkaff	681
Analysis on Energy Utilization of the Key Energy-Consuming Industries in Jiangxi Province Y. Meng, Y. Hu and C.C. Wei	688
Ensuring Reliability of Lithium-Ion Batteries for Space Applications Using Functional Shape Memory Materials Z.M. Blednova and N.A. Protsenko	693
Benchmarking Economical Efficiency of Renewable Energy Power Plants: A Data Envelopment Analysis Approach C. Lo Storto and G. Ferruzzi	699
The Optimization Model of Wind Power and Thermal Power Jointly Run under the TOU Price L.W. Ju, Z.F. Tan, H. Yin and Z.H. Chen	705
Benefit Evaluation Model of Multi-Mode Power Exchange A.Y. Dong, Z.F. Tan, L.W. Ju, Z.H. Chen and H. Xin	711
An Engineering Method of Modeling and Simulation of Photovoltaic P. Luo and X.F. Lv	716
Energetic Analysis of Solar-Supplied Processes for Methane, Biogas and Wood Chip Production F. Cotana, F. Rossi, A. Nicolini, M. Filippini and A.L. Pisello	720
Battery Management System Based on Virtual Instrument X.J. Li, D. Liu, R. Yan, Y.Q. Gong and Y. Pan	725
An Ultra Low Voltage Resonant Converter for Thermoelectric Energy Harvesting S.Z. Guo, K. Xie, Y.H. Ye and X.P. Li	731

Computational Fluids Dynamics Performances Analysis of Ramie-Albizia Composit for Wind Turbine Rotor	
S. Sono, P. Wanto and J.W. Soedarsono	735
Research on Ingot Casting Process and Properties of Poly-Silicon	
B.T. Zhao, W.X. Gao and C.C. Jia	739
A Review on Pitch Angle Control Strategy of Variable Pitch Wind Turbines	
C. Tan and H.H. Wang	744

Chapter 8: Energy Reserves and Geoenvironmental Applications

Utilizing of <i>In Situ</i> Combustion Process in Xinjiang Oil Field through Analysis of Produced Fluids	
J.M. Zhang, X.D. Wu, S.D. Li, J. Zhang, H.H. Zhang, B.L. Qi and Z.Y. Zhong	751
Feasibility Analysis of Fractured-Horizontal Well Development in HuaQing Ultra-Low Permeability Reservoir	
S.Y. Mo, S.L. He, S. Wang, H.Y. Zhang, L.J. Chang and G. Lei	755
Principles of Unsaturated Flow in Tight Gas Reservoirs	
Z.K. Lv, D.H. Gu, S.L. He, H.Y. Zhang and S.Y. Mo	761
The Geochemical Characteristics of Constant Elements of Red Mudstones in the Lower Part of the Fourth Member of Shahejie Formation in Dongying Depression	
L. Liu and N.H. Zhu	765
Application of Absorption and Attenuation Analysis Based on Pre-Stack Seismic Data: Su-77 Block Gas Field Example	
T. Cao and S.B. Guo	771
Coalbed Methane (CBM) Project Enrichment Area and Economic Evaluation	
J.S. Li, Z.X. Li and B.H. Zu	776
Decline Curves of a Vertical Well in Stress-Sensitive Reservoir	
Z. Zhang, S.L. He, H.Y. Zhang, S.Y. Mo and S. Li	781
Research on Types of Oil Reservoirs and Character of Oil-Water Distribution in Heidimiao Layer	
G.Y. Lv	789
Research Progress on Hydrate Self-Preservation Effect Applied to Storage and Transportation of Natural Gas	
Y.G. Wen, Q.X. Chen, Y.W. Chen and S.S. Fan	795
Study on Stress Sensitivity in Microfracture Ultra-Low Permeability Reservoir	
H.Y. Zhang, S.L. He, G.H. Luan, S.Y. Mo, Z.K. Lv and G. Lei	802
Research of Rod Pump Load Reducing Technology on Deep Wells	
X.Q. Cen, X.D. Wu, G. Lei and S.Q. Ma	808
Applicability of Classical Permeability Estimation Models Based on NMR Logging in Tight Sandstones	
D.F. Wei, X.P. Liu and X.X. Hu	814
Seismic Response Analysis of the Tank by Base Isolation	
Y. Yu, L. Wang and Y.F. Zhang	819
Application of Wavelet Transform in High-Resolution Sequence Stratigraphic Division	
D.W. Ji, J. Li and G.D. Lu	823

Chapter 9: Environmental Science and Engineering

Environmental Impact Assessment for Zhonghang Housing Development in Huidong County of Guangdong	
J.S. Yang and X.H. Zhong	831
An Assessment of Comfort Levels of Buildings with Shaded and Non-Shaded Windows in Warm Humid Climates	
O.O. Odim	835
Permanence of a Predator-Prey System with Beddington-DeAngelis Functional Response	
T. Wu	839

Study on Sedimentary Characteristics of Zhang Jia Po Group, Gushi Hollow of Weihe Basin	
L. Zhang, J.C. Liu, X.Y. Wang and J.F. Bai	844
Isolation of Hydrogen-Producing Bacteria Suitable for Immobilization from Anaerobic Sludge	
T. Nomura, H. Asano, T. Takayama, A. Naimen, H. Tokumoto and Y. Konishi	849
Effect of Grassland Degradation on Arbuscular Mycorrhizal Symbiosis of <i>Leymus chinensis</i> (Trin.) Tzvel. in Different Steppe Types	
E. Wu, L.H. Bai and L.X. Cao	855
Influence of Curing Condition and Clay Content on Strength of Geopolymer Soils	
K. Hyugmoon, H.H. Min, N. van Chanh and L.A. Tuan	858
Study on the Role of LEDs in Vegetable Growing in Xingtai Area	
P.Y. Chen, H.L. Hu, L.J. Liang, Z. Li and S.X. Li	863
Generation Resource Planning Optimization Model under Emission Constraint	
S. Lei, Z.F. Tan, L.W. Ju, H. Yin and Z.H. Chen	868
Analysis on the Driving Force of China's Rural Land Circulation	
H.X. Zhang, Y.M. Xu and M.S. Dong	872
Harmonious Development of Urbanization and Water Environment - A Case Study of Wuhan City, China	
L. Hu	878
Preparation of Liquid Ferrate and the Optimization of Process Parameters	
X.H. Sun, L. Wang, W.C. Li and W.Q. Tuo	884

Application of Modified CANDLE Burnup to Very Small Long Life Gas-cooled Fast Reactor

Fiber Monado^{*1,2,a}, Zaki Su'ud^{1,b}, Abdul Waris^{1,c}, Khairul Basar^{1,d},
Menik Ariani^{1,2,e}, Hiroshi Sekimoto^{3,f}

¹Nuclear Physics and Biophysics Research Group, Dept. of Physics, Faculty of Mathematics and Natural Sciences, Bandung Institute of Technology, Bandung, Indonesia

²Dept. of Physics, Faculty of Mathematics and Natural Sciences, Sriwijaya University, Indonesia

³CRINES, Tokyo Institute of Technology, O-okoyama, Meguro-ku, Tokyo 152-8550, Japan

^afiber.monado@gmail.com, ^bszaki@fi.itb.ac.id, ^cawaris@fi.itb.ac.id, ^dkhbasar@fi.itb.ac.id,
^emenikariani@students.itb.ac.id, ^fhsekimot@gmail.com

Keywords: Modified CANDLE, Gas-cooled Fast Reactor, Metallic Fuel, Natural Uranium, Long life fast reactor

Abstract. Gas-cooled Fast Reactor is a good candidate for fourth generation nuclear power plant that projected to be used started in 2030. In this study, modified CANDLE burn-up strategy is adopted to create 300 MWt long life Gas-cooled Fast Reactor with metallic fuel U-10wt%Zr without enrichment. This design demonstrated excellent performance with the average discharge burn-up is about 25.9% HM.

Introduction

Gas-cooled Fast Reactor (GFR) is a high-temperature, helium-cooled fast reactor with a closed fuel cycle. GFR is a good candidate for fourth generation nuclear power plant that projected to be used started in 2030 [1,2]. It combines the reliability of fast spectrum systems and high temperature systems. The fast spectrum were able to use more sustainable sources of uranium and minimizing waste through burning of actinides and fuel recycling. High temperature produces high-thermal cycle efficiency and heat generated is used for industry (to produce hydrogen).

CANDLE (stands for Constant Axial shape of Neutron flux, nuclide densities, and power shape During Life of Energy production) burnup strategy since published in 2000/2001 [3], has been extensively studied by many researchers in Japan and other countries [4-11].

In this research a feasibility design study of very small 300 MWt GFR which can utilize natural uranium as fuel cycle input has been investigated. Modified CANDLE burn-up scheme is adopted to obtain the capability of consuming natural uranium as fuel cycle input [6,7,9,12-14].

Core Model and Calculation Method

This design adopted modified CANDLE burn-up scheme for adjustment fuel in the reactor core. In this design the reactor core is divided into 10 regions with the same volume in the axial direction (see Fig.2). Each region is filled with fuel with different content. In the first cycle of burn-up region-1 which contains fresh fuel (natural uranium) is placed near the region-10 which contains the active fuel. After the first cycle of burn-up (10 years of burn-up) it means enter the second cycle of burn-up: fuel from the region-1 is shifted to the region-2, fuel from region-2 shifted to region-3, fuel from the region-3 is shifted to the region-4, fuel from region-4 is shifted to the region-5, fuel from region-5 is shifted to the region-6, fuel from region-6 is to shifted region-7, fuel from region-7 is shifted to the region-8, fuel from region-8 is shifted to region-9, fuel from region-9 is shifted to region-10, and fuel from the region-10 removed from the reactor core, then region-1 is replenished with fresh fuel.

The calculation is done using the SRAC code system; PIJ and CITATION module [15] with the principal parameters in Table 1 and description sample cases shown in Table 2. PIJ-SRAC module is used for the calculation of burn-up of fuel cell. At the beginning of the calculation, the data for the power density level is the result of assumptions and then done calculations using this data. The result are eight energy group macroscopic cross section data to be used in two dimensional R-Z geometry multi groups diffusion calculation in CITATION-SRAC module. The average power density in each region resulted from the diffusion calculation is then brought back to PIJ-SRAC module for cell burn-up calculation. The iteration is repeated until a convergence condition.

Table 1. Sample design parameter

Parameter	Value/Description
Power (MWt)	300
Number of equal volume region	10
Fuel Material	U-10wt%Zr
Cladding Material	Stainless Steel
Coolant Material	Helium
Fuel Volume fraction	60%
Cladding Volume fraction	10%
Coolant Volume fraction	30%
Active core diameter	220 cm
Active core height	280 cm
Reflector radial width	50 cm
Reflector axial width	50 cm
Pin pitch	1.4 cm
Sub cycle length	10 years
Reactor life	100 years

Table 2. Sample description

Sample case	Description
Case A	Parameter described in Table 1
Case B	Similar to the Case A but power thermal is 275
Case C	Similar to the Case A but power thermal is 250

Results and Discussion

In this study we perform the calculation for the reactor core with a sample design parameters as shown in Table 1 and 2. The parameters survey results of the calculation are the values of effective multiplication factor, infinite multiplication factor, relative power density, burn-up level, intergral conversion ratio, and atomic density discussed in this section.

Fig.3 shows the effective multiplication factor (k-eff) change during burn-up for one cycle of operation over the past 10 years from the reactor core that is designed. The value of k-eff that obtained at the beginning of the cycle is approximately 1.013(critical condition) after that monotonically increases until the end of the cycle(k-eff = 1.042).

Fig.4 shows relative power density axial distribution and its change during 10 years of burn-up in the beginning of cycle(BOC) till the end of cycle(EOC). Mesh number 1 through 30 are active core while the mesh 31 to 40 is the axial reflector. Mesh number 1-3 associated with region 1, mesh number 4-6 associated with the regions 10, mesh number 7-9 associated with the region 9, and so on. Fig.4 is shown peaking factor in EOC decreased compared to BOC, which means that the power distribution becomes more flat.

Fig.5 shows the change of burn-up level during 100 years fuel history in the core. This figure shows the burn-up level at the beginning of life increased slowly until the middle of life, but after that the burn-up level increases rapidly until the end of life. The burn-up level at the end of life is about 259166 MWd/ton HM or about 25.92% HM.

Fig.6 shows the infinite multiplication factor, and the integral conversion ratio change during burn-up history. Sharp increase of the infinite multiplication factor (k_{inf}) value occurs at beginning of life due to the region 1(fresh fuel) located near the region 10(see Fig.2) which contains a lot of fissile material. The k_{inf} value continue to increase until it reaches a maximum value of 1.287 at 74th year burn-up history. After that k_{inf} value decreases slowly until the end of life due to the accumulation of fission product and significantly reduced the amount of U-238.

The conversion ratio value drop about 63% at the beginning of life (the first 10 years) due to the accumulation of plutonium so that the ratio of fertile material to fissile material is significantly reduced. The conversion ratio value decreases slowly after the middle of life until the end of life also due to reduction of fertile material inventory.

Fig.7 shows the Pu-239 and the U-238 atomic density change during burn-up history. The Pu-239 increased significantly at the beginning of reactor operation (10th burn-up history) due to fresh fuel that fills the region-1 is located near the region-10 which contains the active fuel. This correlated with a reduction of U-238 that produced Pu-239 during burn-up. The accumulation of plutonium continues until it reaches the maximum value at the 74th burn-up history and after that decreases.

Figs.8-12 show the results for cases A, B and C. It is shown in Fig.8 that k_{eff} change during burn-up for the case A is higher than in the cases B and C, apparent also that in the case C not achieved critical condition. Figs.9 and 10 show the k_{inf} and the PU-239 atomic density changes during burn-up for the cases A, B and C. It is shown that the most important differences among them appear from about 30th – 70th year of burn-up history. The values of k_{inf} and the Pu-239 atomic density grows faster than cases B and C. However the case A, after the 80th year of burn-up history its values decreases faster than the other cases. Fig.11 shows the U-238 atomic density change during burn-up history for case A, B and C. It is shown that decreases of the U-238 atomic density occurs faster on the case of A than B and C. Fig.12 shows the burn-up level change of fuel during its burn-up history for cases A, B and C. It is shown that burn-up levels are higher for case A than the others. These are consistent with the different power level among the cases A, B and C.

Conclusion

The conceptual design study of 300 MWt long life GFR with natural U-10%wtZr as fuel cycle input has been performed. The reactor discharge burn-up is about 25.9% HM for case A. The present investigation showed that the design of these reactors can operate for 10 years without refueling and fuel shuffling and just need natural uranium as fuel cycle input.

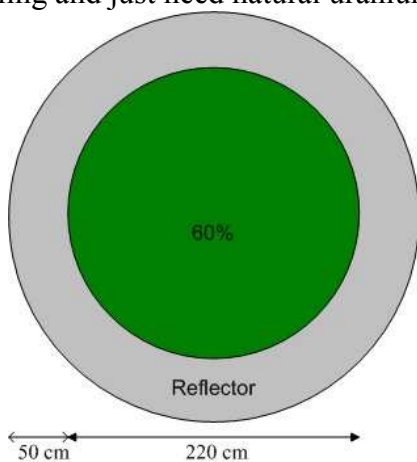


Fig.1 Cross section view of core

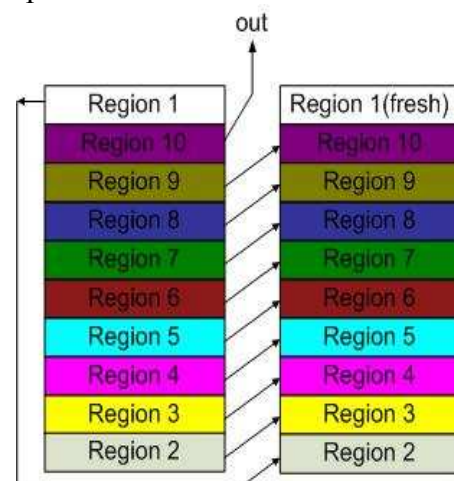


Fig.2 Region division and shuffling using Modified CANDLE burn-up scheme

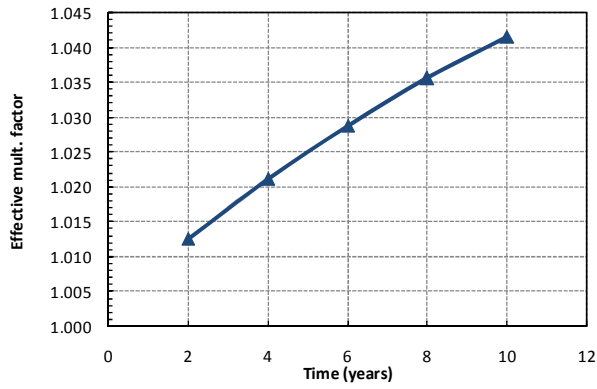


Fig.3 Effective multiplication factor change during burn-up.

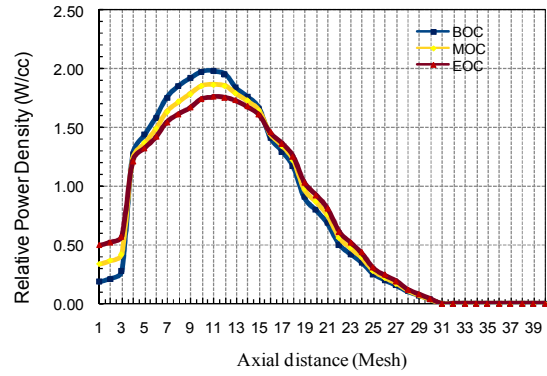


Fig.4 Relative power density axial distribution and its change during 10 years of burn-up.

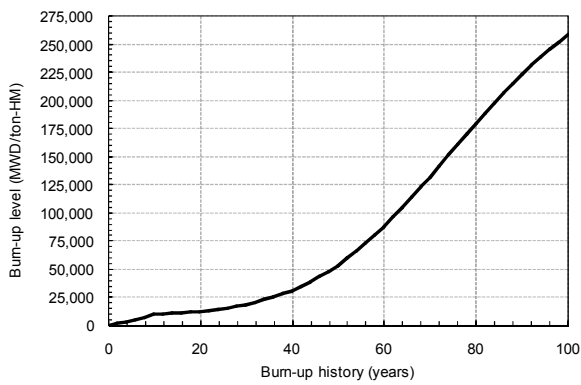


Fig.5 Burn-up level change during burn-up history

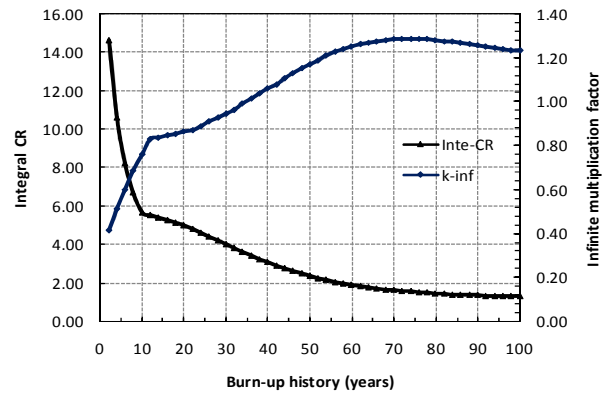


Fig.6 Integral conversion ratio (left), and k-inf change during burn-up history(right)

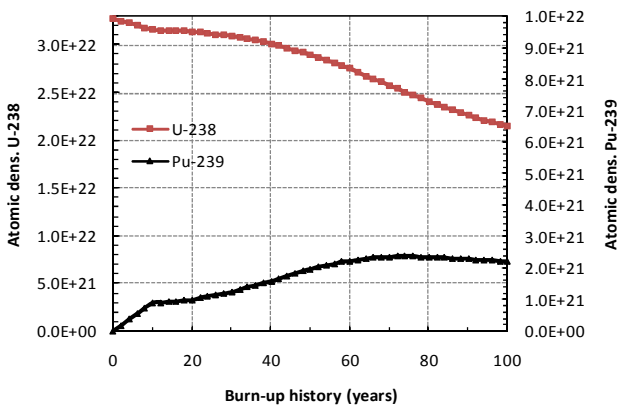


Fig.7 Pu-239 and U-238 atomic density change during burn-up history

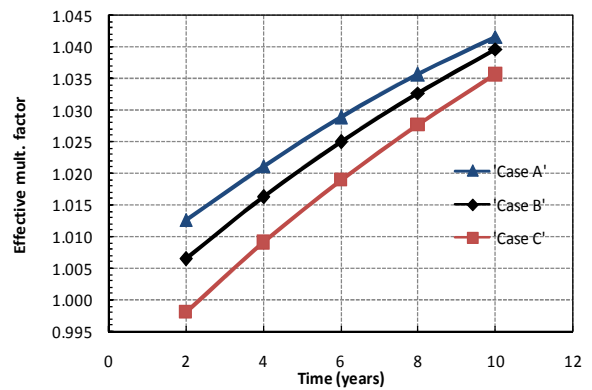


Fig.8 Effective multiplication factor change during burn-up for case A, B, and C

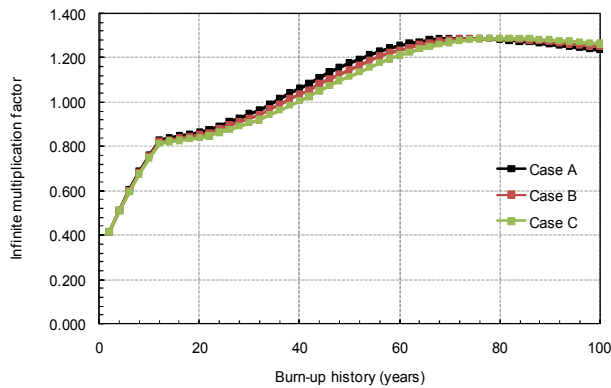


Fig.9 Infinite multiplication factor change during burn-up for case A, B, and C

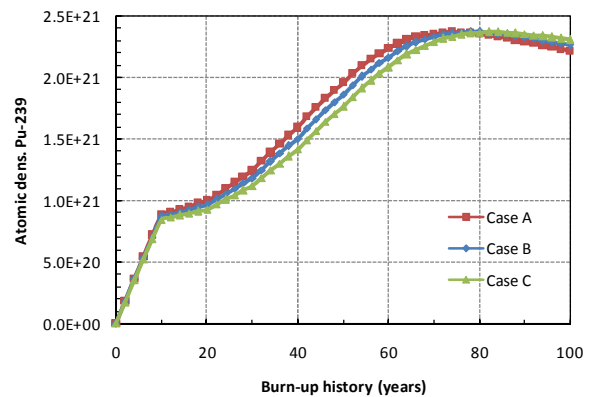


Fig.10 Pu-239 atomic density change during burn-up history for case A, B, and C

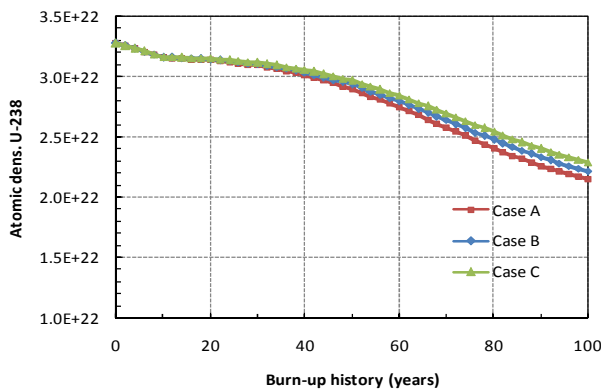


Fig.11 U-238 atomic density change during burn-up history for case A, B, and C

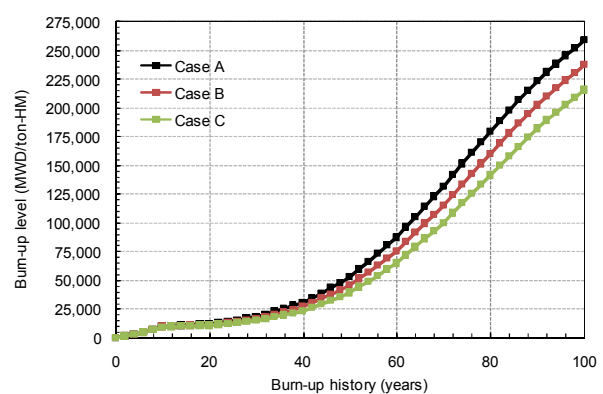


Fig.12 Burn-up level change of fuel during its burn-up history for case A, B, and C

References

- [1] T.Y.C. Wei and K.D. Weaver: Initial Requirements for Gas-Cooled Fast Reactor (GFR) System Design, Performance, and Safety Analysis Models. (Gen IV Nuclear Energy System, INEEL/EXT-04-02242, 2004)
- [2] Information on <http://www.gen-4.org>
- [3] H. Sekimoto, K. Ryu and Y. Yoshimura: Nuclear Science Engineering, 139(2001), p.306
- [4] H. Sekimoto: Recent Research Activities on CANDU Burnup. ICANCE 2007 conference. Bandung, Indonesia(2007).
- [5] A. Nagata, N. Takaki and H. Sekimoto: *Annals of Nuclear Energy* 36(2009), p.562
- [6] Z. Su'ud and H. Sekimoto: *Int. J. Nuclear Energy Science and Technology*, Vol 5, No.4(2010), p.347
- [7] Z. Su'ud and H. Sekimoto: *Annals of Nuclear Energy*, 54(2013), p.58
- [8] M. Ariani, Z. Su'ud, A.Waris, Khairurrijal, F. Monado, H. Sekimoto and S. Nakayama: *American Institute of Physics Conf. Proceeding*, vol. 1454(2012), p. 69
- [9] M. Ariani, Z. Su'ud, F. Monado, A.Waris, Khairurrijal, I. Arif, F. Aziz and H. Sekimoto: *Applied Mechanics and Materials*, Vol. 260-261(2013), p.307
- [10] T. Okawa, S. Nakayama and H. Sekimoto: *Energy Conversion and Management*, 53(2012), p.182
- [11] M.K. Saadi, A. Abbaspour and A. Pazirandeh: *Annals of Nuclear Energy* 50(2012), p.44

- [12] Z. Su'ud and H. Sekimoto: Modified CANDLE burnup scheme and its application for long life Pb-Bi cooled fast reactor with natural uranium as fuel cycle input. ICANCE 2007 conference. Bandung, Indonesia(2007).
- [13] Z. Su'ud and H. Sekimoto: Optimization of modified CANDLE burn-up scheme based long life Pb-Bi cooled fast reactor with natural uranium as fuel cycle input. PBNC 2008 conference, October 11–18, Aomori, Japan(2008).
- [14] M. Ariani, Z. Su'ud, A.Waris, Khairurrijal, N. Asiah and M.A. Shafii: American Institute of Physics Conf. Proceeding, vol. 1325(2010), p. 249
- [15] K. Okumura, T. Kugo, K.Kaneko and K. Tsuchihashi: *SRAC2006: A Comprehensive Neutronic Calculation Code System*, JAEA-Data/Code 2007-004, Reactor Physics Group, Nuclear Science and Engineering Directorate, Japan Atomic Energy Agency (2007).